Hardness of high-pressure high-temperature treated single-walled carbon nanotubes

S. Kawasaki[*],

Department of Materials Science and Engineering, Graduate School of Engineering, Nagoya Institute of Technology, Gokiso-cho, Showa-ku, Nagoya 466-8555, Japan

Y. Nojima, T. Yokomae, F. Okino, H. Touhara,

Faculty of Textile Science and Technology, Shinshu University, 3-15-1 Tokida, Ueda 386-8567, Japan

Abstract

We have performed high-pressure high-temperature (HPHT) treatments of high quality single-walled carbon nanotubes (SWCNTs) over a wide pressure-temperature range up to 13 GPa - 873 K and have investigated the hardness of the HPHT-treated SWCNTs using a nanoindentation technique. It was found that the hardness of the SWCNTs treated at pressures greater than 11 GPa and at temperatures higher than 773 K is about ten times greater than that of the SWCNTs treated at low temperature. It was also found that the hardness change of the SWCNTs is related to the structural change by the HPHT treatments which was based on synchrotron x-ray diffraction measurements.

Key words: carbon nanotubes; high pressure; nanoindentation; x-ray diffraction
PACS: 61.10.Nz; 61.48.+c; 62.50.+p; 68.60.Bs

1 Introduction

Due to their extraordinary physical properties, both fullerenes and carbon nanotubes have attracted much interest. It is well known that the bulk modulus of the C_{60} molecule has been calculated to be 843 GPa [1], which is much greater than that of diamond (441 GPa), and that many theoretical studies of single-walled carbon nanotubes (SWCNTs) give axial Young's modulus values in the Tera Pa range [2]. Therefore, it is expected that new hard materials can be constructed by fullerenes and/or SWCNTs. In the past decades, Blank et al. [3–6] performed the high-pressure high-temperature (HPHT) treatments of C_{60} over a wide pressure-temperature range and reported that HPHT-treated C_{60}s have significantly high hardnesses. The hard phase of the HPHT-treated C_{60}, which becomes hard enough to scratch the (111) face of diamond, was called ultra-hard C_{60}. On the other hand, it was shown by Popov et al. [7] that SWCNTs are also transfromed into a hard phase by inducing a high pressure at room temperature using a diamond anvil cell (DAC). However, HPHT treatments of SWCNTs whose hardnesses have already been reported are limited to restricted pressure-temperature conditions. Therefore, it is meaningful to perform HPHT treatments under several HPHT conditions especially at high temperature in order to explore the new hard phase of SWCNTs. In this study, we have carried out HPHT treatments of well-crystallized SWCNTs under several conditions and compared the hardness of the HPHT-treated SWCNTs with those of diamond and ultra-hard C_{60}.

* fax:+81-52-735-5221

 Email address: `kawasaki.shinji@nitech.ac.jp` (S. Kawasaki).

2 Experimental

The SWCNT sample used in the present study was prepared by the laser ablation method. The Raman spectrum of the SWCNT sample with strong G-bands at about 1590 and 1560 cm^{-1} and a weak D-band at about 1330 cm^{-1} indicates the high quality of the sample (Fig. 1). It was also confirmed by XRD measurment that the sample has a well-crystallized bundle structure (Fig. 2).

The HPHT treatments of the SWCNTs were performed using a cubic anvil press installed at a synchrotron x-ray beamline AR-NE5C of the High Energy Accelerator Research Organization (KEK) in Tsukuba, Japan. In situ XRD measurements under high pressure were performed in order to observe the structural change in the SWCNTs by the HPHT treatments. A boron nitride capsule in which a SWCNT sample was charged was inserted into the center of the pressure-transmitting medium consisting of a mixture of amorphous boron and epoxy resin. The generated pressure was determined from the unit cell parameter of NaCl using Decker's equation of state.

The hardness measurements of the HPHT-treated SWCNTs were performed using the nanoindentation system (Elionix ENT-1100) with a trigonal pyramid Berkovich diamond indenter. The HPHT-treated SWCNT sample having a diameter of 1.0 mm and height of 0.5 mm was fixed by a synthetic resin on a stainless steel sample holder. The sample surface was mirror polished. The indentation measurements were then carried out at 10 different surface points on each sample. The maximum load was set at 500 mgf.

3 Results & Discussion

The angular dispersive XRD (AD-XRD) pattern shown in Fig. 2 can be assigned as the diffractions of the two-dimensional hexagonal lattice of the SWCNTs. The lattice parameter a and tube diameter R were determined to be 1.74 nm and 0.71 nm, respectively, by the simulation of the XRD pattern assuming the SWCNT form factor using the 0th order cylindrical Bessel function (Fig. 2). The determined tube diameter is consistent with the values evaluated by the radial breathing mode (RBM) peak positions in the Raman spectrum (Fig. 1). The closest tube-tube gap was calcualted to be 0.32 nm, which is comparable with the layer distance of graphite and the closest C_{60}-C_{60} gap in the face-centered cubic C_{60}.

For convenience, an SWCNT sample HPHT-treated at x GPa and at y K is abbreviated S-xGPa-yK in this paper. The energy-dispersive XRD (ED-XRD) patterns of the HPHT-treated SWCNT samples are shown in Fig. 3. The patterns were observed at room temperature under atmospheric pressure after the HPHT treatments. The changes in the diffraction patterns with increasing pressure and with increasing temperature are shown elsewhere [8]. It should be noted that the diffraction intensity of each peak in the ED-XRD is apparently quite different from that in the AD-XRD because the diffraction intensity in the ED-mode is much affected by the energy dependence of the brilliance of the incident x-ray photon and of the absorption by the high-pressure cell.

Both S-12GPa-293K and S-13GPa-473K showed almost the same diffraction pattern as the starting SWCNT sample except for the decrease in the (10) diffraction peak intensity due to the increase in absorption of the low energy x-ray by the deformed high-pressure cell [8]. Therefore, they retain their initial structures even

4

after the HPHT treatment. On the other hand, since the diffraction pattern of S-13GPa-873K is completely different from those of S-12GPa-293K and S-13GPa-473K, the structure of S-13GPa-873K should be transformed from the initial structure by the HPHT treatment. The diffraction patterns of both S-7GPa-773K and S-11GPa-773K (not shown) are quite similar to that of S-13GPa-873K, and the pattern of S-11GPa-293K (not shown) is almost the same as that of S-13GPa-293K.

Fig. 4 shows the force-depth indentation curves. Although the indentation curve is not always the same as shown in Fig. 4 even in the same sample at different measurement points, the curves shown in Fig. 4 are typical examples for each sample. The plastic modification hardness was determined using these curves as follows.

$$H_v = P_{\max}/A \qquad (A = 3^{\frac{3}{2}} \tan^2 \alpha h_1^2 / \sin \alpha) \tag{1}$$

where $P_{\max}$ is the maximum load (= 500 mgf), A is the contact surface area of the indenter at depth h_1, and α is the polyhedral angle of the indenter (=65°). The inset in Fig. 4 illustrates $P_{\max}$ and h_1. The obtained hardness, which is the average of 10 sampling points on each sample, is summarized in Table 1.

As shown in Fig. 4, the observed indentation curves are classified into two groups, i.e., the low and high strain curves. The low strain curves are observed for the samples heat-treated at high temperatures (S-13GPa-873K and S-11GPa-773K). The hardness of the sample heat-treated at low temperature does not change from the pristine sample even if the sample is compressed at a high pressure. This result is consistent with the XRD measurements which reveal that no structural change completely occurs by the low-temperature treatment at high pressure. On the other hand, S-8GPa-773K, whose diffraction pattern is completely different from the initial pattern, does not become harder. Therefore, not only the temperature, but also

5

the pressure is an important factor for the hardness change.

Blank et al. [9] investigated the pressure-temperature (p-T) phase diagram of C_{60}. We have used information from the p-T phase diagram to prepare an ultra-hard C_{60} by the HPHT treatment at 13 GPa and 873 K. Fig. 5 shows the indentation curves of diamond (100), the ultra-hard C_{60}, and S-13GPa-873K. The hardness of S-13GPa-873K is significantly less than those of the ultra-hard C_{60} and diamond. The ultra-hard C_{60} is considered to consist of 3-dimensionally networked C_{60} molecules connected by covalent bonds. The structure of the ultra-hard C_{60} was then described as "strongly interacting agglomerates of C_{60} molecules" or a "collapsed fullerite". Although the detailed structure of S-13GPa-873K is still unknown, some chemical bonds between tubes might be introduced similar to the ultra-hard C_{60} because the diffraction lines from the bundle structure disappeared. Unlike the isotropical spherical C_{60} molecule, however, in the case of the SWCNT, it should be noted that the bound SWCNTs might have a significant unisotropy. It is then expected that the bound SWCNTs do not show a high stiffness for the force in the direction perpendicular to the tube axis. This should be the reason why the hardness of S-13GPa-873K is much less than that of the ultra-hard C_{60}.

4 Acknowledgement

References

[1]   R. S. Ruoff, A. L. Ruoff, Nature 350 (1991) 663.

[2]   A. Krishnan, E. Dujardin, T. W. Ebbesen, P. N. Yianilos, M. M. J. Treacy, Phys. Rev. B 58 (1998) 14013.

[3]   V. Blank, M. Popov, S. Buga, V. Davydov, V. N. Denisov, A. N. Ivlev, B. N. Mavrin, V. Agafonov, R. Ceolin, H. Szwarc, A. Rassat, Phys. Lett. 188 (1994) 281.

[4]   V. D. Blank, S. G. Buga, N. R. Serebryanaya, G. A. Dubitsky, R. H. Bagramov, M. Y. Popov, V. M. Prokhorov, S. A. Sulyanov, Appl. Phys. A 1997; 64: 247-250.

[5]   V.D.Blank, V.N. Denisov, A.N. Ivlev, B. N. Mavrin, N. R. Serebryanaya, G. A. Dubitsky, S.N. Sulyanov, M. Yu. Popov, N.A. Lvoya, S.G.Buga, G.N. Kremkova, Carbon 36 (1998) 1263.

[6]   V. D. Blank, S. G. Buga, N. R. Serebryanaya, G. A. Dubitsky, B. N. Mavrin, M. Y. Popov, R. H. Bagramov, V. M. Prokhorov, S. N. Sulyanov, B. A. Kulnitskiy, Y. V. Tatyanin, Carbon 36 (1998) 665.

[7]   M. Popov, M. Kyotani, R. J. Nemanich, Y. Koga, Phys. Rev. B 65 (2002) 033408-1.

[8]   S. Kawasaki, Y. Matsuoka, T. Yokomae, Y. Nojima, F. Okino, H. Touhara, H. Kataura, Carbon 43 (2005) 37.

[9]   V. D. Blank, S. G. Buga, G. A. Dubitsky, N. R. Serebryanaya, M. Yu Popov, B. Sundqvist, Carbon 36 (1998) 319.

Table 1

Hardness values of HPHT-treated SWCNTs, diamond, graphite and ultra-hard C_{60} determined by nanoindentation.

sample	HPHT treatment		Plastic modification
	Pressure (GPa)	Temp. (K)	hardness (mgf/μm^2)
S-8GPa-773K	7.9	773	25.1(6.9)
S-11GPa-293K	10.9	293	27.7(3.8)
S-11GPa-773K	10.7	773	292.3(51.6)
S-12GPa-293K	12.4	293	20.0(0.7)
S-13GPa-473K	12.9	473	22.6(8.0)
S-13GPa-873K	12.6	873	365.4(59.6)
Diamond (100)	–	–	7724(409)
Ultra-hard C_{60}	13.5	873	2144(957)
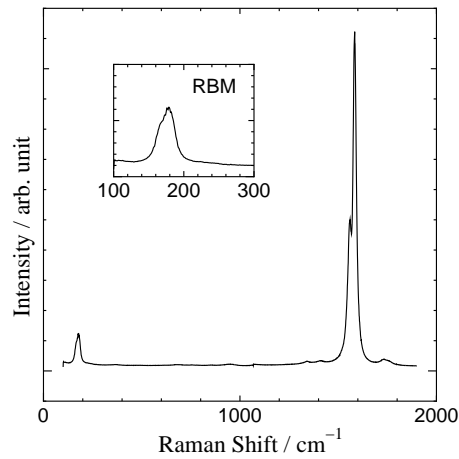
Fig. 1. Observed Raman (Ar laser: 514.5 nm) spectrum of pristine SWCNT sample.
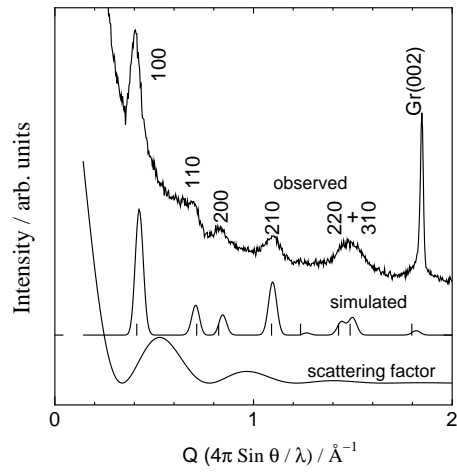
Fig. 2. A comparison between the observed and simulated XRD patterns of pristine SWCNT sample. Gr(002) denotes the 002 diffraction line of the graphite impurity. Vertical tick marks are the calculated Bragg positions.
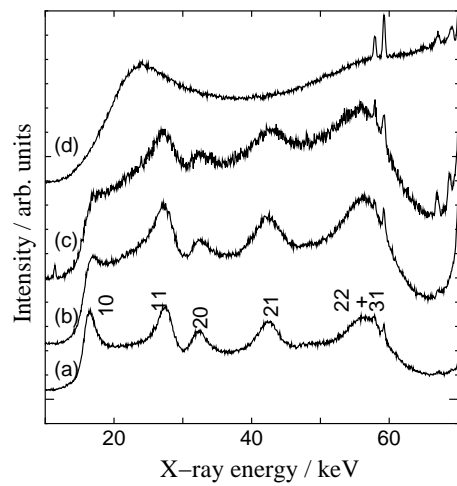
Fig. 3. Energy-dispersive XRD patterns of (a) pristine SWCNT sample, (b) S-13GPa-293K, (c) S-13GPa-473K, and (d) S-13GPa-873K. The detector angle was set at $2\theta = 3°$.
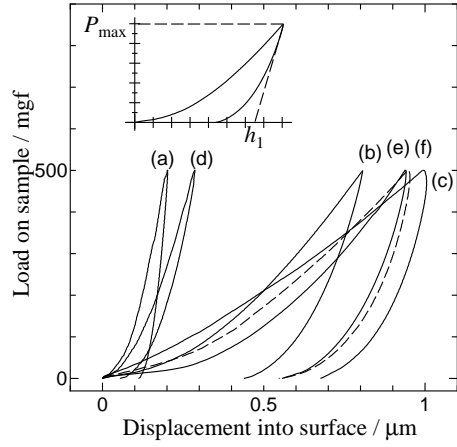
Fig. 4. Force-depth indentation curves of (a) S-13GPa-873K, (b) S-13GPa-473K, (c) S-13GPa-293K, (d) S-11GPa-773K, (e) (solid line) S-11GPa-293K, and (f) (dashed line) S-8GPa-773K.
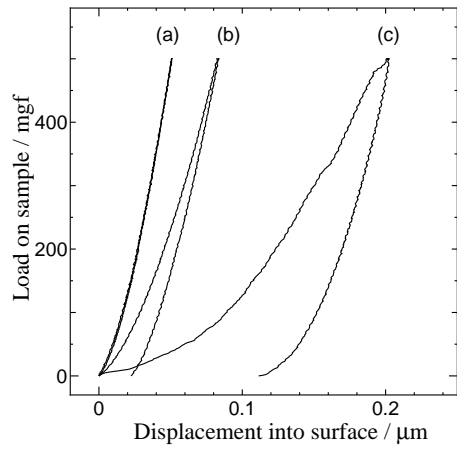
Fig. 5. Force-depth indentation curves of (a) diamond (100), (b) super-hard C_{60}, and (c) S-13GPa-873K.